The effects of disturbance on the microbial mediation of sediment stability

Naiyu Zhang[1, 2*], Charlotte E.L. Thompson[2, 3], and Ian H. Townend[2]

[1]State Key Laboratory of Marine Geology, Tongji University, Shanghai, China

[2]School of Ocean and Earth Science, National Oceanography Centre, University of Southampton, Southampton SO14 3ZH, U.K.

[3]Channel Coastal Observatory, National Oceanography Centre, Southampton, SO14 3ZH, U.K.

*Corresponding author: Naiyu Zhang (21310078@tongji.edu.cn)

Charlotte E.L. Thompson: celt1@noc.soton.ac.uk

Ian H. Townend: I.Townend@soton.ac.uk

Key words: Biofilm, disturbance, bioturbation, bio-stabilization, bio-destabilization, biofilm-sediment aggregates, bio-sediment formation

Abstract

In coastal areas, biofilms are often subject to disturbance by hydrodynamic forcing, bioturbation and human activities. These factors affect the influences biofilms have on the sediment. To reveal these effects, we studied laboratory-incubated and field-collected biotic sediments reworked by disturbances, and examined their stabilities and three-dimensional microstructures using laboratory annular flume tests and a wet-staining X-ray Microcomputed tomography (μ-CT) method. We find that, when subject to disturbance, biofilms do not always establish mat-like matrices that firmly armour the seabed and bio-stabilize sediments, but instead, have a range of effects on sediment stability, including both bio-stabilization and destabilization. Disturbance considerably alters microbial influences on sediment stability, but is not the only control. Given equal disturbance, whether or not sediments are bio-stabilized largely depends on the state of bio-sediment formation. At a relatively well-developed state, an organic-rich, adhesive polymer network tightly interconnects large amounts of sediment particles into aggregates, forms complex internal structures, and enhances sediment stability. By contrast, some bio-sediment formations only ever reach a less well-developed state, where scattered organic patches bind relatively few particles into aggregates and reduce sediment stability. Microbial growth likely has two opposing effects on sediment stability, by enhancing either weight/friction or lift/drag on aggregated particles. The former has the positive effect of enhancing sediment stability, whereas the latter can result in greater flow resistance and so have the opposite effect. A conceptual framework is put forward to characterize the different

states of bio-sediment formation and their distinct effects on sediment stability.

Introduction

The solid-liquid interfaces of aquatic sediment particles provide preferential habitats for microbial cells to colonise and grow. These microbial cells do not live as single dispersed cells (Probandt et al. 2018), but instead, through the secretion of sticky organic matter (e.g. extracellular polymeric substances (EPS)), attach to the surfaces of sediment particles, building up adhesive biofilm structures and accumulating additional microbe cells, sediment grains and particles (Decho 2000; Flemming and Wingender 2010; Sutherland 2001). Heterogeneous and porous three-dimensional (3D) aggregated microstructures of large diversity, ranging from small clusters, large flocs, to multi-layered biofilm mats of varying thickness are formed (Flemming 2019); i.e., biofilm-sediment aggregates (BSAs) (Zhang et al. 2018).

The ubiquitous presence of biofilm and bio-sediment formation alters the physical transport of sediment (Fang et al. 2020; Malarkey et al. 2015; Mariotti and Fagherazzi 2012). Studies acknowledge that the mat matrices of biofilm can suppress sediment resuspension, by both binding sediment particles into an adhesive organic mat, which provides an adhesive force that armours the bed, and also by smoothing bed roughness to reduce drag, thus enhancing sediment stability; i.e. ‘biostabilization’ (Paterson et al. 1989; Friend et al. 2008; Parsons et al. 2016).

A tightly-bound, mat-like matrix, however, is not always established. Coastal areas are dynamic, with disturbances including hydrodynamic forcing, such as currents and waves, bioturbation caused by zoobenthos, and human activities such as footprints, dredging and fishing trawls (Michaud et al. 2005; Foden et al. 2011; Thompson et al. 2017). Such disturbances prevent the successful establishment of biofilm mats, a process that takes several days (Chen et al. 2017; Gerbersdorf et al. 2008; Vignaga et al. 2013), rather they tend to form patchy, loosely-connected, diffusive and fluffy biofilm matrices (Hope et al. 2020; Orvain et al. 2014). BSA that is disturbed as it develops may be of more relevance in dynamic coastal seas (Mariotti et al. 2014; Mariotti and Fagherazzi 2012).

Two contrasting effects of disturbance have been noted on biofilm development: (1) biostabilization remains after cyclic resuspension and deposition (Friend et al. 2003a; Hope et al. 2020), in which disturbance did not degrade bio-stabilization and strong bio-stabilization was rapidly restored after a few cycles of moderate disturbance, even though distinct transport behaviours were observed relative to biofilm mats (Chen et al. 2019). Such rapid restoration of biostabilization occurs during spring-neap tidal cycles (Van De Koppel et al. 2001; Mariotti & Fagherazzi 2012). In contrast, (2) the destabilization of sediments by microbial development (i.e., bio-destabilization) has been reported when the coastal areas are dominated by intense and frequent disturbances caused by factors such as storm, waves and bioturbation (Amos et al. 2004; Le Hir et al. 2007; Orvain et al. 2003). In these cases, the concentrations of microbial substances (e.g. chlorophyll *a* and EPS concentrations) negatively correlate with bed stability (erosion thresholds) (Hope et al. 2020; Orvain et al. 2014; Thompson, et al. 2017).

It is likely that intense and frequent disturbances do not allow the mat matrices of biofilms and their strong bio-stabilization effects to establish/restore, but instead generate an alternative state with a less well-developed bio-sediment formation that reduces sediment stability (Van De Koppel et al. 2001; Mariotti and Fagherazzi 2012). Such a state occurs during the initial stages of biofilm incubation. Within hours of initial bio-sediment formation, the attachment of dispersed microbial aggregates aids the motion of sand grains (Mariotti et al. 2014). At the early stage of microbial development, a rapid increase in field biomass reduces the critical shear stresses for sediment erosion (De Brouwer et al. 2005).

This work addresses the following question: *Do biofilms always enhance sediment stability when subject to disturbance, or do they have a range of effects, including bio-destabilization?*

We hypothesized that sediment disturbance has a range of effects on microbial influences on sediment stability, including both enhancing and reducing sediment stability (bio-stabilization and destabilization). Further we hypothesized that bio-destabilization is a relatively less well-developed state of bio-sediment formation. To test this latter hypothesis, the resuspension thresholds of biotic sediments developed under physical disturbances were examined using laboratory flume tests. The 3D microstructural features of these disturbed biotic sediments were directly captured by μ-CT scans, to reveal the states of bio-sediment formation.

Materials and Methods

The creation and collection of biotic sediments

Biotic sediments were cultured in the laboratory using single algae species, and collected from tidal flats colonized with natural microbial assemblages. By applying different hydrodynamic disturbance regimes, two types of biotic sediment were created during a 6-day incubation period: a fluffy sediment-water interface created under daily resuspension disturbance referred to as ‘fluff’, and a mat-like sediment-water interface created in calm waters with no disturbances referred to as ‘mat’. Surface intertidal sediments were collected, transported back to the laboratory and hand mixed to fully rework/disturb the sediments before the experiments (sediment sampling and preparation are detailed below). Two types of field sediments with different abiotic matrices were tested; one comprising of predominantly silty sediment, whilst the other was a sandy sediment.

Laboratory-created biotic sediments

Biotic sediments were created in an annular flume, the Core Mini Flume (CMF) (Thompson et al., 2013), over a 6-day incubation period. A flat sediment surface was hand-moulded, with a sediment depth of 6 cm overlaid with 15 cm depth of artificial sea water (Sigma sea salts, salinity 35 ppt). The sediment was comprised of fine-grained sand sieved to the range of 125-250 μm with a d_{50} = 195 μm, acid washed in advance to remove organic matter. Slurries of algae clay aggregates provided the microbial source and were cultured using a single species of diatom, *Phaeodactylum tricornutum* (cultured in the Research Aquarium Laboratory, National Oceanography Centre, Southampton), and kaolinite clays (ACROS Organics^{TM}), following the protocols of Zhang et al. (2018). They were added into the flume and allowed to settle overnight on the sand before the 6-day period of incubation started.

The mat was allowed to grow under quiescent flow conditions with no hydrodynamic disturbance for 6 days. The fluff was created in an identical CMF with the same experimental setting, except that daily cycles of resuspension (6 hours) and deposition (18 hours) were applied at a constant shear stress of 1.0 Pa that exceeds the resuspension thresholds of sand grains for 6 days. In both treatments the sediments were kept illuminated for 24 h at 18 ºC, and oxygenated through air stones 24 h per day, to keep the microbe cells alive.

Two replicates were run for each treatment, with one for the resuspension threshold test, and the other for μ-CT experiments (Figure S1). Triplicate resuspension tests were conducted on the fluff, to examine the reliability of the experimental results of resuspension thresholds.

Field-collected biotic sediments

To determine whether similar results occur for natural microbial assemblages, field samples were collected from two sampling sites ~ 200 m apart in the Tay estuary, Scotland (56º26'42" N, 2º52'11" W) at the end of October in 2019. The Tay estuary is a macrotidal, 50-km long coastal embayment on the east coast of Scotland, UK. At each site, the top ~10 mm of the sediments were sampled for microphytobenthos and their organic products, which were placed in plastic boxes with ice bags under dark conditions and transported back to laboratories immediately after sampling (~12 h). Samples were kept in a fridge at 4 ºC under dark conditions for one week. The samples were then hand mixed and homogenized to fully disturb and rework the sediments, which were remoulded into a plane bed in the CMFs and gently overlaid with 15 cm depth of artificial seawater (salinity 35 ppt). The CMFs were allowed to settle overnight before experimentation, and kept at 18 ºC, illuminated and oxygenated, to create consistent environmental conditions with the laboratory-created sediments. According to Folk's classification (Folk, 1954), the samples from site 1 belong to sandy silt (sand fraction = 47%, d_{50} = 60 μm, and d_{50} of sands = 98 μm) and are referred to as silty sediments. Samples taken from site 2 belong to silty sand (sand fraction = 63%, d_{50} = 120 μm, and d_{50} of sands = 239 μm), and are referred to as sandy sediments.

The silty and sandy field sediments were prepared in two identical CMFs, with one used for resuspension threshold test, and the other for μ-CT experiments.

Resuspension experiments

Resuspension experiments were performed in the CMFs (Thompson et al., 2013) (Figure S1(a)), which is a small worktop annular flume (Amos et al., 1992). It consists of two 5 mm-thick acrylic tubes; an outer diameter of 200 mm and inner diameter of 110 mm, which leaves a 40 mm-wide working channel in which a sediment bed can be formed. An Optical Backscatter Sensor (OBS) was placed at 4 cm above the bed at the same height as a sampling port, for measuring suspended sediment concentration. A Nortek Vectrino Acoustic Doppler Velocimeter (ADV) was used to measure flow velocity at 6 cm above the sediments (Figure S1(a)). Steady currents were generated by 4 equidistant motor-controlled paddles, the speed of which was computer controlled (Thompson et al., 2004; 2013). Stepwise increased motor speeds were programmed and time steps of 10-minute were used to suspend the biotic sediments. (Amos et al., 2004; Amos et al., 1992; Thompson et al., 2003; 2011). OBS data was calibrated against the measured concentration of suspended materials (g/L) sampled from the same height as the OBS every 2-3 velocity steps (Thompson et al., 2013). Suspension samples for OBS calibration were taken using a 50 ml plastic syringe and filtered through 47 mm GF/F Whatman filter. The filters were then oven dried at 60 ºC and weighed to calibrate the OBS data. The suspended concentrations during the stepwise increased resuspension tests were obtained.

Bed shear stress was estimated using the turbulent kinetic energy method (TKE) (Amos et al., 2004; Thompson et al., 2003), which measures the intensity of turbulent motions within a shearing fluid and calculates the turbulent kinetic energy density, *E*, from the spectrum of a velocity time series: $E=\frac{1}{2}\rho_w(\overline{u}_t^2+\overline{v}_t^2+\overline{w}_t^2)$ (where ρ_w is water density, u_t, v_t,and w_t are flow velocity fluctuations in stream-wise, cross-stream and vertical directions) (Soulsby, 1997; Thompson et al., 2004). The bed shear stress can be calculated according to $\tau_b = 0.19E$ (Soulsby, 1997). The resuspension threshold was determined by plotting the bed shear stresses against the suspended sediment concentration (Amos et al., 2004; Sutherland et al., 1998).

μ-CT experiments

A wet staining method was used to scan the 3D structures of the BSA (Zhang et al., 2018), and this varied according to the sample composition. For samples comprised of fine-grained clay particles (e.g. the BSA suspended from the fluff sediments at moderate flow intensities), samples were collected from the sampling port during the resuspension process using a 20 ml syringe and stained using absolute alcohol and Alcian Blue dye solution (Sigma; 0.4 wt%/wt at pH 2.5), following Zhang et al. (2018). The μ-CT scans of the treated specimens were conducted using a Zeiss 160 kVp Versa 510 X-ray microscope, at the *μ*-VIS X-ray Imaging Centre, University of Southampton (Figure S1(b)). A high resolution of 0.7 × 0.7 ×0.7 μm was achieved.

A modified method was used for sand grains, which can be two orders of magnitude larger than clay minerals, requiring a considerably larger field of view provided by the modified 225 kVp Nikon HMX ST, housed at the same facility. In this case, samples were collected using a 50 ml syringe corer and placed in a sealed glass vessel that was topped up with absolute alcohol and Alcian Blue dye solution (Sigma;0.4 wt%/wt at pH 2.5). After an overnight treatment, the sediments of the top ~3 cm in the syringe core was sectioned using a steel knife, which was carefully washed and rinsed using distilled water and ethanol in succession. The sectioned layer of the sediments was subsampled using borosilicate Nuclear Magnetic Resonance (NMR) tubes (Norell™ Standard Series™; outer diameter 4.9 mm, inner diameter 4.2 mm, depth 20 mm), by inserting the tube into the sectioned sediment layer. After the sub-sampling, wet staining liquid (absolute alcohol and Alcian Blue dye solution) was gently added into the tube, to ensure the sampled BSA remained in a hydrated state.

The NMR tubes were then sealed using NMR caps and sealing parafilm, in order to avoid potential evaporation and desiccation during the scanning process. Each scan at HMX took approximately 1 hour and the resulting voxel resolution was 4.5 $\times$ 4.5 $\times$ 4.5 µm. 3D microstructures including the number of adhered sand grain, organic matter content, 3D volume and surface area, and volume equivalent diameter, as well as the BSA density profiles were quantified by a pre-developed protocol using CT-pro, Image J and Avizo 9.3.0 (Callow et al., 2018; Zhang et al., 2018).

Results

Microbial mediation of sediment resuspension thresholds

Resuspension tests were conducted on the laboratory-created fluff and mat, and the field-collected silty and sandy sediments. The results were compared against their theoretical abiotic thresholds, to examine microbial effects on sediment stability.

Laboratory-created sediments

The suspended concentrations vs. the shear stresses for clean sand, the mat and fluff are shown in Figure 1. The threshold for suspending abiotic clean sand grains into the water column obtained from the control tests was 0.84 Pa (Figure 1 (a)), consistent with empirical threshold estimate of 0.85 Pa, using Roe (2007)'s empirical relationship (Table S1, Eq. (S1) in the SI).

Both the mat and fluff present a two-stage resuspension process, initiated at different thresholds (Figure 1 (b-c)). An examination of suspended materials during the first stage showed no sand grains, with only organic-rich materials suspended (stage 1), while considerable suspension of sand grains occurred in the second stage (stage 2). μ-CT examination confirmed that the suspended materials from stage 1 primarily consisted of aggregates of organic matter and kaolinite clays (no sand grains), hence reflecting the microbial influences on the stability of clay particles. According to annular flume tests by Mehta and Partheniades (1982) (where the same clay mineralogy, water salinity, measurement techniques and methods were considered), the resuspension threshold of abiotic kaolinite clays after 24 h consolidation is 0.21 Pa. This measurement is consistent with the theoretical threshold estimate of 0.22 Pa obtained using Wu et al. (2018)'s formula (Table S1, Eq. (S2) in the SI). Our experiments showed the biofilm-mediated clays were not suspended until the applied shear stresses reached 0.43 Pa (stage 1 of the mat, Figure 1(b)) and 0.31 Pa (stage 1 of the fluff, Figure 1(c)). The shear stress threshold value for the resuspension of clay particles from the mat is clearly greater than that of the fluff, suggesting a rather larger effect of bio-stabilization for the clay particles in the mat when biofilm development was not disturbed. The less significant biostabilization effects for the clay particles in the fluff is likely caused by the periodic disturbances. Nevertheless, the biofilm that was disturbed as it developed stabilized clay particles.

In stage 2, the entrainment of sand grains occurred at 0.94 Pa for the mat, which is higher than that of clean sand (0.84-0.85Pa), implying a bio-stabilization effect. By contrast, the suspension of sand grains from the fluff occurred at an applied shear stress of 0.74 Pa, which is lower than that of clean sand. Hence the disturbed biofilm development destabilized the sand grains.

Previous examination notes the standard errors of CMF measurement are in the range 0.01-0.03 Pa (Thompson et al., 2013). Taking the upper bound of the error, the resuspension threshold of clay BSAs from the fluff is 0.31 ± 0.03 Pa, higher than the theoretical thresholds of 0.21-0.22 Pa, supporting clay BSAs as bio-stabilizers. The resuspension threshold of fluff BSAs is 0.74 ± 0.03 Pa, lower than the abiotic threshold of 0.84-0.85 ± 0.03 Pa, while mat BSAs have a higher resuspension threshold of 0.94 ± 0.03 Pa, supporting fluff BSAs as bio-destabilizers and mat BSAs as bio-stabilizers. In calm waters, mat matrices of biofilm can rapidly establish and stabilize sediments. By contrast, when the biofilm growth was disturbed, such that no mat matrices were able to become established, the response is more complex, with the fine fraction (clay) exhibiting biostabilization and the coarse fraction (sand) destabilization. Hence disturbance seems unlikely to be the only control and other mechanisms must have an influence.

Field-collected sediments

In contrast to the laboratory sediments, no clear two-stage resuspension processes were observed for the silty and sandy sediments collected in the field. This is likely because the sediments were hand-mixed and homogenised before the test, and some of the naturally occurring fluffy material were lost through collection. During the short period of settlement, no distinguishable two-layered matrices formed at the bed. Plots of the suspended concentrations against the shear stress during the step-wise increased resuspension tests showed that the entrainment of silty and sandy field sediments started at 0.44 Pa and 1.05 Pa, respectively (Figure 1 (d)).

Theoretical thresholds for the suspension of abiotic sand-mud mixtures were calculated. No direct measurements were taken, due to the unknown resuspension/deposition history of the sediments in the field and thus the challenges of successfully replicating the packing of sediment particles in the field. Five commonly cited empirical relationships that have been developed and tested for a variety of sediment properties, measurement techniques, and analysis methods, were used to obtain abiotic threshold estimates (Eq. (S3-S7) in Table S1 of the SI) (Ahmad et al., 2011; Van Ledden, 2003; Van Rijn, 1993; 2007; Wu et al., 2018; Yao et al., 2018). The theoretical threshold estimates of abiotic sand-mud mixtures are in the range of 0.12-0.30 Pa for the silty mixtures, and 1.55-2.46 Pa for the sandy mixtures.

The consideration of the CMF measurement errors of 0.03 allows a clear separation between bio-stabilization and destabilization. The biofilm-mediated field silty sediment entered water at a shear stress of 0.44 ± 0.03 Pa, higher than their abiotic threshold estimates of 0.12-0.30 Pa, indicating an enhanced sediment stability by disturbed biofilms (Figure 1(d-e)). By contrast, the entrainment of the biofilm-mediated sandy field sediment occurred at 1.05 ± 0.03 Pa, lower than their theoretical abiotic threshold estimates of 1.55-2.46 Pa, indicating a reduced sediment stability by disturbed biofilms (Figure 1(d-e)). The consistent results from our laboratory-created and field-collected sediments suggest that, whilst the establishment of a biofilm mat, such as that developed in calm waters, enhances sediment stability as previously acknowledged, both bio-stabilization and destabilization can develop when subject to disturbance (Figure 1(e)).

3D microstructural features of biofilm mediated sediments

μ-CT experiments were conducted to examine the 3D microstructural features of biofilm mediated sediments. In total, five types of material were examined. This includes the suspended materials during stage 1 from the fluff, but excluded the suspended materials during stage 1 from the mat, as the large pieces of the suspended material could not be extracted from the flume port. For the fluff and mat, after the organic-rich and loosely-attached materials were removed during stage 1, the materials remaining on the bed were examined. The materials at the surface of the silty and sandy field sediments were also examined using μ-CT. Figure 2 (1a-5c) illustrates 3D views of the microstructures of the five types of material, and their microstructural properties are summarized in Table S3.

The materials suspended during stage 1 from the fluff are comprised of aggregates formed by organic matter and clay particles, referred to as clay BSA (Figure 2 (1a-c)). Extensive, relatively well-developed networks of organic matter tightly adhere large amounts of clay particles, forming organic rich microstructures at a relatively well-developed state (high organic fraction: 0.78 ± 0.09).

After the removal of clay BSA during stage 1, distinct BSA matrices remain in the fluff (Figure 2 (2a-c)) and the mat (Figure 2 (3a-c)). In the fluff, organic matter form discrete and scattered patches, attaching to relatively few sand grains in poorly-structured aggregates, coined fluff BSA (Figure 2 (2a-c)). These aggregates appear to be at much less well-developed states, of relatively low organic fraction (0.20 ± 0.07). By contrast, BSAs in the mat developed in calm waters have copious amounts of organic matter and developed an aggregate with multilayer structures, tightly adhered to large numbers of sand grains, and coherently bind into mat matrices of biofilm, referred to as mat BSA (Figure 2 (3a-c)). As a result, the mat BSAs contain a significantly higher organic matter fraction (0.55 ± 0.04), 2-3 times higher than that of the fluff BSA, which enables the adherence of an order of magnitude larger number of sand grains into larger aggregates.

3D imaging illustrates distinct BSA microstructures at the silty and sandy field sediments. Whilst both were reworked by disturbances, the organic matter from the silty field sediments appears to be relatively well-developed into an adhesive organic polymer network, where large amounts of fine-grained sediment particles were adhered and embedded into tightly structured aggregates, coined field silty BSA (Figure 2 (4a-c)). By contrast, in the reworked sandy field sediments, the state of bio-sediment formation appears to be less well-developed. A few coarse sand grains are attached by discrete biofilm patches and small amounts of fined-grained sediment particles, coined field sandy BSA (Figure 2 (5a-c)). The field sandy BSAs contain a significantly lower organic fraction (0.15 ± 0.05), 5-6 times lower than that of field silty BSAs (0.80 ± 0.06).

When disturbed, the aggregates that enhance sediment stability (bio-stabilizers: clay and field silty BSAs) and reduce sediment stability (bio-destabilizers: fluff and field sandy BSAs) established significantly different and distinguishable 3D microstructures in terms of their constituent make-up and geometry (Figure 2 (6a-c)). The bio-stabilizers were at a relatively well-developed state of bio-sediment formation, where the biofilm managed to build an extensive and cohesive organic polymer network, resulting in a high organic to sediment ratio (organic fraction = 0.78 ± 0.08, Figure 2 (6a)). Large amounts of sediment grains are tightly interconnected, establishing highly complex internal structures with high porosities and irregularities (porosity = 0.87 ± 0.07, roundness = 0.13 ± 0.08, Figure 2 (6b-c)). Sediments are bio-stabilized. By contrast, the organic network in the bio-destabilizers shows a less well-developed state, constituting a significantly lower organic fraction (organic fraction = 0.18 ± 0.07, $p < 0.001$, Figure 2 (6a),), building less complex internal structures with significantly lower porosities and surface irregularities (porosity = 0.67 ± 0.10, roundness = 0.37 ± 0.10, $p < 0.001$, Figure 2 (6b-c)). Sediment stability is reduced. As such, BSA microstructures formed at different states of bio-sediment formation play a key role in mediating sediment stability.

Discussion

Entrainment process of biofilm mediated sediments: the effects of disturbance

In calm waters, armouring matrices of biofilm mat develop (Figure 3 (1a)). At the surface of the mat, some relatively young, randomly-developed branches of organic matter may loosely connect with the mat and protrude into the flow (Droppo et al. 2007; Flemming 2019). These therefore experience stronger bed shear stresses than the planar areas of the mat, and were easily detached in stage 1 at a moderate applied shear stress (Figure 3 (1b)). This has been observed by others (Chen et al. 2019), and is likely due to the non-uniform development of the biofilm (Jesus et al.

2005). However, the loss of these protrusions does not eliminate the overall mat stability. The armouring matrix of the mat retains its integrity and so continues to protect the sediments. If this were not the case, the underlying sand grains would enter the water column at their abiotic threshold shear stress of 0.84 Pa, which did not occur. The immobilised sand grains also prevent bed-load transport. Once the applied flow shear stress exceeds the "weakest" adhesion between the mat BSA and the underlying sediment bed, the local integrity of the mat matrix is lost (Chen et al. 2019; Vignaga et al. 2013). The underlying material is exposed to the flow at a higher shear stress than the clean sand entrainment threshold (Figure 3 (1c)), causing immediate mass resuspension of the bed sediments in an "all-or-nothing" fashion (Le Hir et al. 2007;. Mariotti and Fagherazzi 2012) (Figure 3 (1d)). Adhesion with the bed predominantly controls and limits entrainment by the biofilm mat (Fang et al. 2014, 2017).

By contrast, a stable biofilm mat is unlikely to develop in the short period between disturbances on the order of hours (Mariotti et al. 2014). Instead, discrete aggregates are formed, developing loose connections with the seabed and presenting a fluffy appearance at the sediment-water interface (i.e., the clay, fluff and sandy and silty field BSAs, Figure 3 (2a)). The adhesion established between biofilm aggregates and the seabed during the short periods between disturbances can be more than 5 times weaker than that for the mat (Fang et al. 2014)(Figure 3 (2b)), and can be broken at lower flow intensities than are needed to directly lift them into water. The detached aggregates are not immediately suspended, but are transported as bed-load, sliding/rolling and saltating on top of sediments before suspension (Figure 3 (2c), and Video SI for the detachment, bed-load transport and suspension of field silty BSAs as an example). Once the balance between the flow lift/drag forcing and submerged BSA weight/friction forcing is reached, BSAs are lifted into the water and sediment entrainment occurs (Figure 3 (2d)). Hence sediment entrainment is not only controlled by adhesive strength, but largely determined by the balance between flow lift/drag and weight/friction forces. If this balance is reached at a shear stress higher than that of abiotic sediments, biofilm stabilizes the sediment, such as in the clay and field silty BSA samples. However, if the balance is reached at a lower applied shear stress that cannot suspend those abiotic sediments, sediments are bio-destabilized, such as for the fluff and field sandy BSA.

Application of Shields parameter to distinguish microbial influences

Multiple criteria have been established to characterize the abiotic thresholds of sediment transport (Shields 1936; Bagnold 1966; Buffington,1999)(abiotic Shields diagram, Figure S2). For example, the Shields parameter, $\theta_{crit,\ S} = \frac{\tau_{crit}}{(\rho_S - \rho_w) g d_{50}}$, and dimensionless particle diameter, $D_{*,S} = (\frac{(\rho_S / \rho_w - 1) g}{\nu^2})^{1/3} d_{50}$ consider the size, d_{50}, and effective density, ρ_S / ρ_w, of clean sediment particles (in which τ_{crit} is the critical shear stress for sediment resuspension, ρ_S and ρ_w are the densities of inorganic sediment particles and water, g is gravitational acceleration and ν is kinematic viscosity of water). In this scenario, sediment matrices with the same particle size and effective density have the same resuspension thresholds, and microbial effects cannot be directly distinguished.

The microbial development has, to different extents, enlarged the size and reduced the density of aggregated particles. Including these differences leads to a more robust interpretation of biofilm mediation. It is possible to define a Shields parameter for the solid matter within the sediment, $\theta_{crit,M} = \frac{\tau_{crit}}{(\rho_M - \rho_w) g d_M}$, and matter dimensionless diameter, $D_{*,M} = (\frac{(\rho_M / \rho_w - 1) g}{\nu^2})^{1/3} d_M$, where ρ_M / ρ_w and d_M are effective density and sizes of the solid matter (organic matter and sediment particles) within the aggregates. (A detailed deviation of ρ_M and d_M are provided in Text S1). These are related through a power law relationship (Figure 4(a)):

$$\theta_{crit,M} = 0.80 D_{*M}^{-0.88},\ R^2 = 0.91 \qquad (1)$$

It is relevant to note that, among the total 78 BSAs tested in this study, only 3 of them are from the mat developed in calm waters, which exhibit a different resuspension mechanism from those in disturbed environments (Chen et al. 2019). The analysis in this section focuses on the 75 disturbed BSAs. The empirically determined suspension thresholds using Eq. (1) fall on or close to the 1:1 line against the thresholds obtained from experiments, showing a reasonable level of agreement, except for the field sandy BSA (Figure 4(b)).

The effects of pore water can be included using a Shields parameter for aggregates, $\theta_{crit,A} = \frac{\tau_{crit}}{(\rho_A - \rho_w) g d_A}$, and the aggregate dimensionless diameter, $D_{*,A} = \left[\frac{(\rho_A / \rho_w - 1) g}{\nu^2}\right]^{1/3} d_A$, where d_A and ρ_A are the densities and sizes of aggregates (including both soild matter and pore water encapsulated within aggregates). A power law relationship was found between $\theta_{crit,A}$ and $D_{*,A}$ in Figure 4 (c):

$$\theta_{crit,A} = 4.3 D_{*A}^{-1.3}, R^2 = 0.77 \qquad (2)$$

The threshold estimates using Eq. (2) are plotted against the experimentally-tested results, showing an overall good level of agreement, though the results appear to be more scattered (Figure 4 (d)). For the field sandy BSA, the agreement is improved compared to the Shields diagram for matter, whereas accounting for pore water has only a small influence on the other BSA (The role of pore water is discussed in Text S2).

The importance of aggregate matter in determining sediment stability is not surprising, given that the properties of BSA matter reflect the states of bio-sediment formation. At a relatively well-developed state, a rapid expansion of BSA size occurs, because more mass is encapsulated and weight/friction forces are enhanced to resist flow erosion. In this case, biofilm development and its aggregation with sediment particles have a positive effect on sediment stability. The bed stability increases with the standing stock of algae cells (chlorophyll *a* concentration) (Le Hir et al. 2007; Sutherland et al. 1998; Thompson et al. 2011), and the amount of their EPS secretions (e.g. colloidal carbohydrate contents) (Friend et al. 2003b; Underwood and Paterson 1993; Yallop et al. 2000), for both sandy and muddy sediments (Hope et al. 2020).

Conversely, BSA expansion needs copious amounts of organic matter to be produced. The increased fraction of organic polymers reduces aggregate bulk density as in the clay and field silty BSA. As bed stability positively correlates with bulk densities of sediments (Amos et al. 1997; Thompson et al. 2013, 2017), a reduction in bulk density caused by microbial development reduces sediment stability, and leads to negative correlations between chlorophyll *a* and/or EPS contents and bed stability (Hope et al. 2020; Orvain et al. 2014; Thompson, et al. 2017). The copious secretion of organic substances glues more sediment particles into larger sizes, enlarging the projected area, making the internal structure more complex and increasing BSA surface roughness (Maggi and Tang 2015). The larger projected area and higher surface roughness cause higher lift/drag forces, making the aggregates less stable to erosion. Consequently, biofilm growth and its aggregation with sediment particles play a negative role on sediment stability.

A conceptual framework for microbial mediation at different states

Whether the sediment stability is enhanced or reduced by bio-sediment formation is more complex than previously thought, and needs to consider the net effects of BSA development. We suggest three important states of bio-sediment formation, with distinct microstructures and influences on sediment transport (Figure 5 (a-d)):

(I) When the time available for bio-sediment formation is short, scattered and discrete patches of organic polymers and colloids attach, coat and bridge relatively few sediment grains, forming poorly-structured 3D aggregates (e.g., fluff and field sandy BSA, Figure 5 (a)). The increase in weight/friction forcing is moderate and easily offset by the negative effects of flow lift/drag forces caused by increased BSA structure complexity, surface roughness and projected area (Figure 5 (d)). The net effect is negative and sediment stability is reduced (bio-destabilization). When subject to erosion, the loose connections between the BSAs and seabed are quickly broken. The BSAs behave akin to single particle grains, starting bed-load transport before suspension (Figure 3(2a-d)).

(II) Continuous cell growth and EPS secretion build up well-structured 3D organic-rich polymer network, tightly binding large amounts of sediment grains, such as our clay and field silty BSA (Figure 5 (b)). However, due to frequent resuspension, the BSAs do not tightly interconnect into a coherent mat armour. Similar to state (I), the adhesion between BSAs and seabed breaks at moderate flow intensities, and BSAs are transported as bed-load before suspension (Figure 3 (2a-d)). In this state, the well-established organic network has a great capacity to encapsulate large amounts of mass, increasing its weight/friction to resist flow erosion and increase bed stability (Figure 5 (b)). The positive effects on sediment stability surpass the negative effects, and sediment stability is enhanced.

(III) With little disturbances, discrete aggregates become tightly interconnected into mat matrices, armouring the underlying sediments (Figure 5 (c)). The mat matrices have a “smoothed” surface roughness and the negative effects on sediment stability are reduced (Figure 5 (d)), resulting a significant effect of biostabilization by a factor ranging from 1.25 to 20 (Amos et al. 1997; Paterson 1989; Yallop et al. 1994). In contrast to states (I) and (II), the “weakest” adhesion between the mat and seabed determines the mass entrainment of sediments, which occurs with surface biofilm failure in an “all-or-nothing” fashion (Decho 2000; Black et al. 2002).

We note that BSA dynamics are influenced by a range of factors, including sediment matrices, microbial species and nutrients. Higher microbial growth and production rates are commonly found in muddy sites, likely due to the high level of nutrients entrapped in interstitial pores and absorbed on the surfaces of these fine grains (Le Hir et al. 2007; Stal 2010). Our work only finds state II for clays and silts. This result agrees with van de Koppel (2001) that silt and clay particles provide a more favourable substrate for diatom growth and promote biostabilization to quickly establish, and less likely to remain in state I compared to sands. Hence the apparent ubiquity of state I for naturally occurring clay and silt substrates is unclear. Further research into the nature and dynamics of microbial influences on sediments is warranted.

Acknowledgement

This work was partially funded by the National Natural Science Foundation of China (Grant No. 42206059), the BLUEcoast project (NE/N 015703/1), and the China Postdoctoral Science Foundation (2021M702472). We gratefully acknowledge Dr. Hachem Kassem for his help in flume setup instructions. We wish to thank Prof. David Paterson and Dr. Andrew Blight at St Andrews University for hosting field sampling work in Scotland. We wish to extend our thanks to Dr. Kathryn Rankin and Dr. Orestis Katsamenis for their assistance in performing the scans carried out at the μ-VIS X-ray Imaging Centre, University of Southampton. We also thank the editor and the two anonymous reviewers for their constructive comments, which makes the manuscript significantly improved.

References

Ahmad, M. F., Dong, P., Mamat, M., Wan Nik, W. B., and Mohd, M. H. (2011). The critical shear stresses for sand and mud mixture. *Applied Mathematical Sciences*, 5: 53–71.

Amos, C. L., Feeney, T., Sutherland, T. F., and Luternauer, J. L. (1997). The stability of fine-grained sediments from the Fraser River delta. *Estuarine, Coastal and Shelf Science*, 45: 507–524. doi:10.1006/ecss.1996.0193

Amos, C. L., and others (2004). The stability of tidal flats in Venice Lagoon - The results of in-situ measurements using two benthic, annular flumes. *Journal of Marine Systems*, 51: 211–241. doi:10.1016/j.jmarsys.2004.05.013

Amos, Carl L., Daborn, G. R., Christian, H. A., Atkinson, A., and Robertson, A. (1992). In situ erosion measurements on fine-grained sediments from the Bay of Fundy. *Marine Geology*, 108: 175–196. doi:10.1016/0025-3227(92)90171-D

Bagnold, R. A. (1966). An Approach to the Sediment Transport Problem from General Physics. *USGS Professional Paper*.

Beaulieu, S. E. (2002). Accumulation and fate of phytodetritus on the sea floor. *Oceanography and Marine Biology,* 40: 171–232. doi:10.1201/9780203180594.ch4

Black, K. S., Tolhurst, T. J., Paterson, D. M., and Hagerthey, S. E. (2002). Working with natural cohesive sediments. *Journal of Hydraulic Engineering*, 128: 2–8. doi:10.1061/(ASCE)0733-9429(2002)128:1(2)

De Brouwer, J. F. C., Wolfstein, K., Ruddy, G. K., Jones, T. E. R., and Stal, L. J. (2005). Biogenic stabilization of intertidal sediments: The importance of extracellular polymeric substances produced by benthic diatoms. *Microbial Ecology*, 49: 501–512. doi:10.1007/s00248-004-0020-z

Buffington, J. M. (1999). The Legend of A. F. Shields. *Journal of Hydraulic Engineering*. doi:10.1061/(asce)0733-9429(1999)125:4(376)

Callow, B., Falcon-Suarez, I., Ahmed, S., and Matter, J. (2018). Assessing the carbon sequestration potential of basalt using X-ray micro-CT and rock mechanics. *International Journal of Greenhouse Gas Control*, 70: 146–156. doi:10.1016/j.ijggc.2017.12.008

Chen, X. D., Zhang, C. K., Paterson, D. M., Townend, I. H., Jin, C., Zhou, Z., and Feng, Q. (2019). The effect of cyclic variation of shear stress on non-cohesive sediment stabilization by microbial biofilms: the role of 'biofilm precursors.' *Earth Surface Processes and Landforms*. doi:10.1002/esp.4573

Chen, X. D., Zhang, C. K., Paterson, D. M., Thompson, C. E. L., Townend, I. H.,

Gong, Z., and Feng, Q. (2017). Hindered erosion: The biological mediation of noncohesive sediment behavior. *Water Resources Research*, 53: 4787–4801. doi:10.1002/2016WR020105
Decho, A. W. (2000). Microbial biofilms in intertidal systems: An overview. *Continental Shelf Research*, 20: 1257–1273. doi:10.1016/S0278-4343(00)00022-4
Droppo, I. G., Ross, N., Skafel, M., and Liss, S. N. (2007). Biostabilization of cohesive sediment beds in a freshwater wave-dominated environment. *Limnology and Oceanography*, 52: 577–589. doi:10.4319/lo.2007.52.2.0577
Fang, H. W., Shang, Q., Chen, M., and He, G. (2014). Changes in the critical erosion velocity for sediment colonized by biofilm. *Sedimentology*, 61: 648–659. doi:10.1111/sed.12065
Fang, H. W., Huang, L., Zhano, H., Cheng, W., Chen, Y., Fazeli, M., and Shang, Q. (2020). *Mechanics of Bio-Sediment Transport*. Springer, Berlin, Heidelberg. doi:10.1007/978-3-662-61158-6
Fang, H. W., Lai, H. J., Cheng, W., Huang, L., and He, G. J. (2017). Modeling sediment transport with an integrated view of the biofilm effects. *Water Resources Research*, 53: 7536–7557. doi:10.1002/2017WR020628
Flemming, H. C. (2019). Bacteria and archaea on Earth and. *Nature Reviews Microbiology*, 17: 247–260. doi:10.1038/s41579-019-0158-9
Flemming, H. C., and Wingender, J. (2010). The biofilm matrix. *Nature Reviews Microbiology*, 8: 623–633. doi:10.1038/nrmicro2415
Folk, R. L. (1954). The Distinction between Grain Size and Mineral Composition in Sedimentary-Rock Nomenclature. *The Journal of Geology*. https://doi.org/10.1086/626171
Friend, P. L., Collins, M. B., and Holligan, P. M. (2003a). Day-night variation of intertidal flat sediment properties in relation to sediment stability. *Estuarine, Coastal and Shelf Science*, 58: 663–675. doi:10.1016/S0272-7714(03)00178-1
Friend, P. L., Ciavola, P., Cappucci, S., and Santos, R. (2003b). Bio-dependent bed parameters as a proxy tool for sediment stability in mixed habitat intertidal areas. *Continental Shelf Research*.23:1899-1917. doi:10.1016/j.csr.2002.12.001
Friend, P. L., Lucas, C. H., Holligan, P. M., and Collins, M. B. (2008). Microalgal mediation of ripple mobility. *Geobiology*, 6: 70–82. doi:10.1111/j.1472-4669.2007.00108.x
Gerbersdorf, S. U., and Wieprecht, S. (2015). Biostabilization of cohesive sediments: Revisiting the role of abiotic conditions, physiology and diversity of microbes, polymeric secretion, and biofilm architecture. *Geobiology*, 13: 68–97. doi:10.1111/gbi.12115
Gerbersdorf, S. U., Jancke, T., Westrich, B., and Paterson, D. M. (2008). Microbial stabilization of riverine sediments by extracellular polymeric substances. *Geobiology*, 6: 57–69. doi:10.1111/j.1472-4669.2007.00120.x
Le Hir, P., Monbet, Y., and Orvain, F. (2007). Sediment erodability in sediment transport modelling: Can we account for biota effects? *Continental Shelf Research*, 27: 1116–1142. doi:10.1016/j.csr.2005.11.016

Hope, J. A., and others (2020). Interactions between sediment microbial ecology and physical dynamics drive heterogeneity in contextually similar depositional systems. *Limnology and Oceanography*, 65: 2403–2419. doi:10.1002/lno.11461

Jesus, B., Brotas, V., Marani, M., and Paterson, D. M. (2005). Spatial dynamics of microphytobenthos determined by PAM fluorescence. *Estuarine, Coastal and Shelf Science*. 65: 30-42. doi:10.1016/j.ecss.2005.05.005

Foden, J., Rogers S. I., and Jones, A. P. (2011). Human pressures on UK seabed habitats: a cumulative impact assessment. *Mar Ecol Prog Ser*, 428: 33–47.doi: 10.3354/MEPS09064

Van De Koppel, J., Herman, P. M. J., Thoolen, P., and Heip, C. H. R. (2001). Do alternate stable states occur in natural ecosystems? Evidence from a tidal flat. *Ecology*, 82: 3449–3461. doi:10.1890/0012-9658(2001)082[3449:DASSOI]2.0.CO;2

Van Ledden, M., Van Kesteren, W. G. M., and Winterwerp, J. C. (2004). A conceptual framework for the erosion behaviour of sand-mud mixtures. *Continental Shelf Research*, 24: 1–11. https://doi.org/10.1016/j.csr.2003.09.002

Le Hir, P., Monbet, Y., and Orvain, F. (2007). Sediment erodability in sediment transport modelling: Can we account for biota effects? *Continental Shelf Research*, 27: 1116–1142. doi:10.1016/j.csr.2005.11.016

Maggi, F., and Tang, F. H. M. (2015). Analysis of the effect of organic matter content on the architecture and sinking of sediment aggregates. *Marine Geology*, 363: 102–111. doi:10.1016/j.margeo.2015.01.017

Malarkey, J., and others (2015). The pervasive role of biological cohesion in bedform development. *Nature Communications*, 6: 2–7. doi:10.1038/ncomms7257

Mariotti, G., and Fagherazzi, S. (2012). Modeling the effect of tides and waves on benthic biofilms. *Journal of Geophysical Research G: Biogeosciences*, 117: 1–14. doi:10.1029/2012JG002064

Mariotti, G., Pruss, S. B., Perron, J. T., and Bosak, T. (2014). Microbial shaping of sedimentary wrinkle structures. *Nature Geoscience*, 7: 736–740. doi:10.1038/NGEO2229

Mehta, A. J., and Partheniades, E. (1982). Resuspension of deposited cohesive sediment beds. *Coastal Engineering*, 1569–1588. doi:10.1061/9780872623736.095

Michaud, E., Desrosiers, G., Mermillod-Blondin, F., Sundby, B., and Stora, G. (2005). The functional group approach to bioturbation: The effects of biodiffusers and gallery-diffusers of the Macoma balthica community on sediment oxygen uptake. *Journal of Experimental Marine Biology and Ecology*, 326: 77–88. doi:10.1016/j.jembe.2005.05.016

Orvain, F., Le Hir, P., and Sauriau, P. G. (2003). A model of fluff layer erosion and subsequent bed erosion in the presence of the bioturbator, Hydrobia ulvae. *Journal of Marine Research*, 61: 823–851. doi:10.1357/002224003322981165

Orvain, F., Guizien, K., Lefebvre, S., Bréret, M., and Dupuy, C. (2014). Relevance of macrozoobenthic grazers to understand the dynamic behaviour of sediment erodibility and microphytobenthos resuspension in sunny summer conditions.

Journal of Sea Research. 92: 46-55. doi:10.1016/j.seares.2014.03.004

Parsons, D. R., Schindler, R. J., Hope, J. A., Malarkey, J., Baas, J. H., Peakall, J., et al. (2016). The role of biophysical cohesion on subaqueous bed form size. *Geophysical Research Letters*, 43: 1566–1573. doi:10.1002/2016GL067667

Paterson, D. M. (1989). Short-term changes in the erodibility of intertidal cohesive sediments related to the migratory behavior of epipelic diatoms. *Limnology and Oceanography*, 34: 223–234. doi:10.4319/lo.1989.34.1.0223

Probandt, D., Eickhorst, T., Ellrott, A., Amann, R., and Knittel, K. (2018). Microbial life on a sand grain: From bulk sediment to single grains. *ISME Journal*, 12: 623–633. doi:10.1038/ismej.2017.197

Van Rijn, L. C. (1993). *Principles of sediment transport in rivers, estuaries and coastal seas*. *Amsterdam: Aqua publications.*

Van Rijn, L. C. (2007). Unified view of sediment transport by currents and waves. I: Initiation of motion, bed roughness, and bed-load transport. *Journal of Hydraulic Engineering*, 133: 649–667. doi:10.1061/(ASCE)0733-9429(2007)133:6(649)

Roe, S. (2007). *A laboratory study of the derivation of the suspensionthreshold of fine and very fine sand*. University of Sounthampton.

Shields, I. A. (1936). Application of similarity principles and turbulence research to bed-load movement, U.S. Soil Conservation Service Coop. Lab. In *Ott, W.P., van Uchelen, J.C. (Eds.), (Translators), Hydrodynamics Laboratory Publication, vol. 167. California Institute of Technology, Pasadena*.

Soulsby, R. L. (1997). *Dynamics of marine sands: a manual for practical applications*. *Dynamics of marine sands: a manual for practical applications*.

Stal, L. J. (2010). Microphytobenthos as a biogeomorphological force in intertidal sediment stabilization. *Ecological Engineering*, 36: 236–245. doi:10.1016/j.ecoleng.2008.12.032

Sutherland, I. W. (2001). The biofilm matrix - An immobilized but dynamic microbial environment. *Trends in Microbiology*, 9: 222–227. doi:10.1016/S0966-842X(01)02012-1

Sutherland, T. F., Amos, C. L., and Grant, J. (1998). The effect of buoyant biofilms on the erodibility of sublittoral sediments of a temperate microtidal estuary. *Limnology and Oceanography*, 43: 225–235. doi:10.4319/lo.1998.43.2.0225

Thompson, C. E. L., Amos, C. L., Jones, T. E. R., and Chaplin, J. (2003). The Manifestation of Fluid-transmitted Bed Shear Stress in a Smooth Annular Flume - A Comparison of Methods. *Journal of Coastal Research*, 19: 1094–1103. doi:10.2307/4299251

Thompson, C. E. L., Amos, C. L., Lecouturier, M., and Jones, T. E. R. (2004). Flow deceleration as a method of determining drag coefficient over roughened flat beds. *Journal of Geophysical Research: Oceans*, 109. doi:10.1029/2001jc001262

Thompson, C. E. L., Couceiro, F., Fones, G. R., Helsby, R., Amos, C. L., Black, K., et al. (2011). In situ flume measurements of resuspension in the North Sea. *Estuarine, Coastal and Shelf Science*, 94: 77–88. doi:10.1016/j.ecss.2011.05.026

Thompson, C. E. L., Couceiro, F., Fones, G. R., and Amos, C. L. (2013). Shipboard measurements of sediment stability using a small annular flume-core mini flume

(CMF. *Limnology and Oceanography: Methods*. 11:604-685. doi:10.4319/lom.2013.11.604

Thompson, C. E. L., Williams, M. E., Amoudry, L., Hull, T., Reynolds, S., Panton, A., and Fones, G. R. (2017). Benthic controls of resuspension in UK shelf seas: Implications for resuspension frequency. *Continental Shelf Research*, 185:3-15. doi:10.1016/j.csr.2017.12.005

Underwood, G. J. C., and Paterson, D. M. (1993). Seasonal changes in diatom biomass, sediment stability and biogenic stabilization in the severn estuary. *Journal of the Marine Biological Association of the United Kingdom*, 73: 871–887. doi:10.1017/S0025315400034780

Vignaga, E., Sloan, D. M., Luo, X., Haynes, H., Phoenix, V. R., and Sloan, W. T. (2013). Erosion of biofilm-bound fluvial sediments. *Nature Geoscience*, 6: 770–774. doi:10.1038/ngeo1891

Wu, W., Perera, C., Smith, J., and Sanchez, A. (2018). Critical shear stress for erosion of sand and mud mixtures. Journal of Hydraulic Research, 56: 96–110. doi:10.1080/00221686.2017.1300195

Yallop, M. L., Paterson, D. M., and Wellsbury, P. (2000). Interrelationships between rates of microbial production, exopolymer production, microbial biomass, and sediment stability in biofilms of intertidal sediments. *Microbial Ecology*, 39:116–127. doi:10.1007/s002489900186

Yallop, M. L., De Winder, B., Paterson, D. M., and Stal, L. J. (1994). Comparative structure, primary production and biogenic stabilization of cohesive and non-cohesive marine sediments inhabited by microphytobenthos. *Estuarine, Coastal and Shelf Science*, 39: 565–582. doi:10.1016/S0272-7714(06)80010-7

Yao, P., Hu, Z., Su, M., Chen, Y., and Ou, S. (2018). Erosion Behavior of Sand-silt Mixtures: the Role of Silt Content. *Journal of Coastal Research*, 85: 1171–1175. doi:10.2112/si85-235.1

Zhang, N., Thompson, C. E. L., Townend, I. H., Rankin, K. E., Paterson, D. M., & Manning, A. J. (2018). Nondestructive 3D Imaging and Quantification of Hydrated Biofilm-Sediment Aggregates Using X-ray Microcomputed Tomography. *Environmental Science and Technology*, 52: 13306–13313. doi:10.1021/acs.est.8b03997

Figures

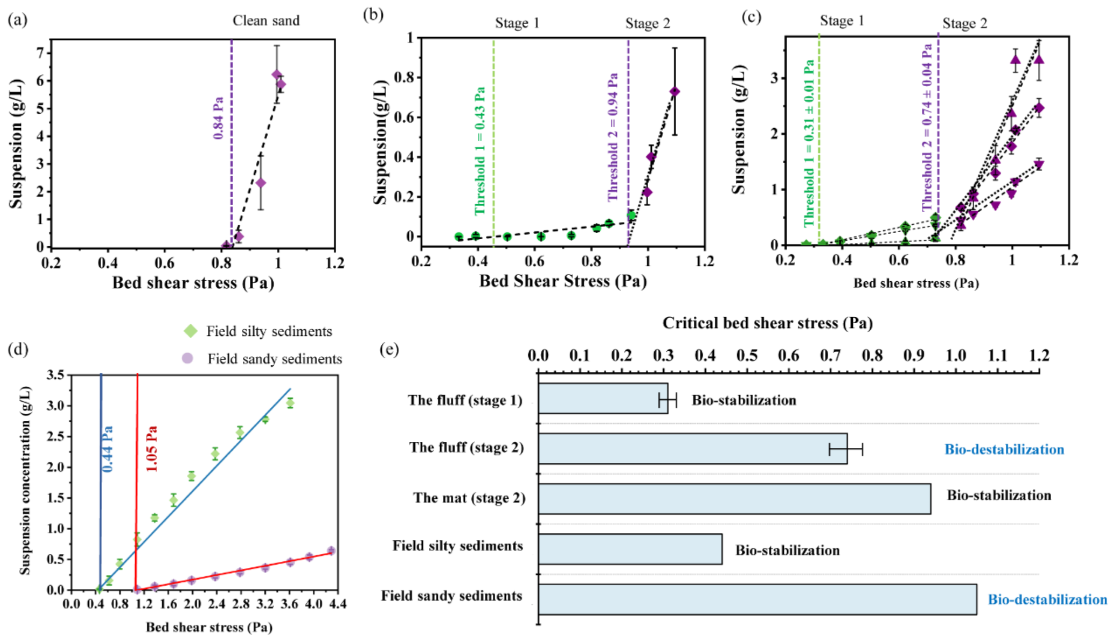

Figure 1. Suspended sediment concentration (g/L) vs. bed shear stress (Pa) for five experimental conditions: abiotic control clean sand (a), mat BSA (b) and fluff BSA (c), silty and sandy field sediments (d), with a summary of the corresponding effects on sediment stability for each in (e). In (c), three replicates for the fluff resuspension experiments are plotted, and each replicate is presented as triangle, diamond, inverted triangle, respectively. Black dashed lines show regression lines of suspension concentration against applied shear stress (a-c). Results are presented as mean ± SD.

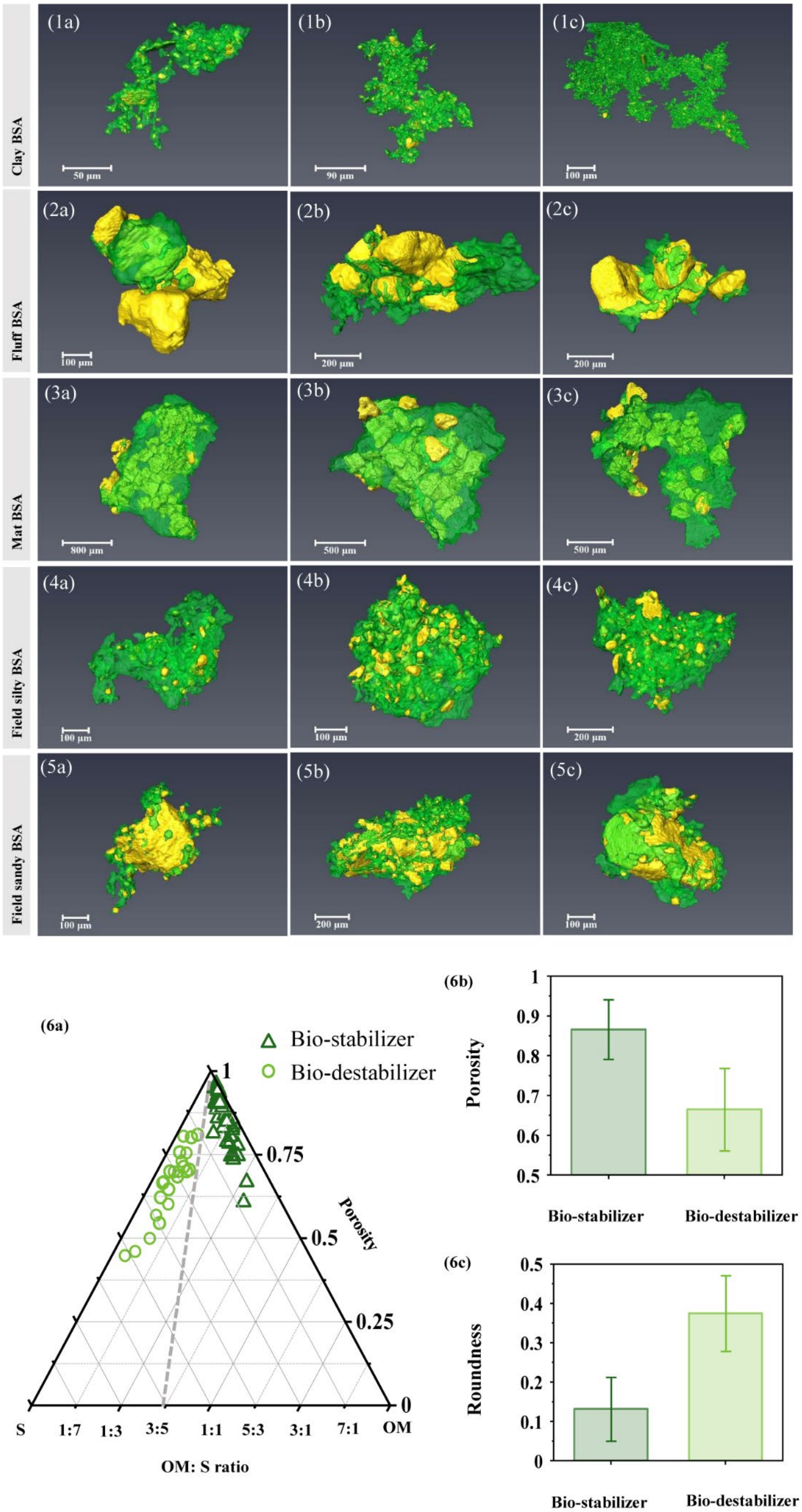

(1a)
(1b)
(1c)
Clay BSA
50 µm
90 µm
100 µm
(2a)
(2b)
(2c)
Fluff BSA
100 µm
200 µm
200 µm
(3a)
(3b)
(3c)
Mat BSA
800 µm
500 µm
500 µm
(4a)
(4b)
(4c)
Field silty BSA
100 µm
100 µm
200 µm
(5a)
(5b)
(5c)
Field sandy BSA
100 µm
200 µm
100 µm
(6a)
Bio-stabilizer
Bio-destabilizer
1
0.75
0.5
0.25
0
Porosity
S
1:7
1:3
3:5
1:1
5:3
3:1
7:1
OM
OM: S ratio
(6b)
Porosity
1
0.9
0.8
0.7
0.6
0.5
Bio-stabilizer
Bio-destabilizer
(6c)
Roundness
0.5
0.4
0.3
0.2
0.1
0
Bio-stabilizer
Bio-destabilizer

Figure 2. μ-CT scans of the 3D microstructures showing states of bio-sediment formation, including clay (1a-c) and the fluff BSAs (2a-c) from the fluff, mat BSAs (3a-c) from the mat, silty (4a-c) and sandy BSAs (5a-c) from the field-collected sediments. Ternary plots of BSA constituent make-up (6a), porosity (6b) and structure roundness (6c) of the bio-stabilizing and destabilizing BSAs. Results are presented as mean ± SD.

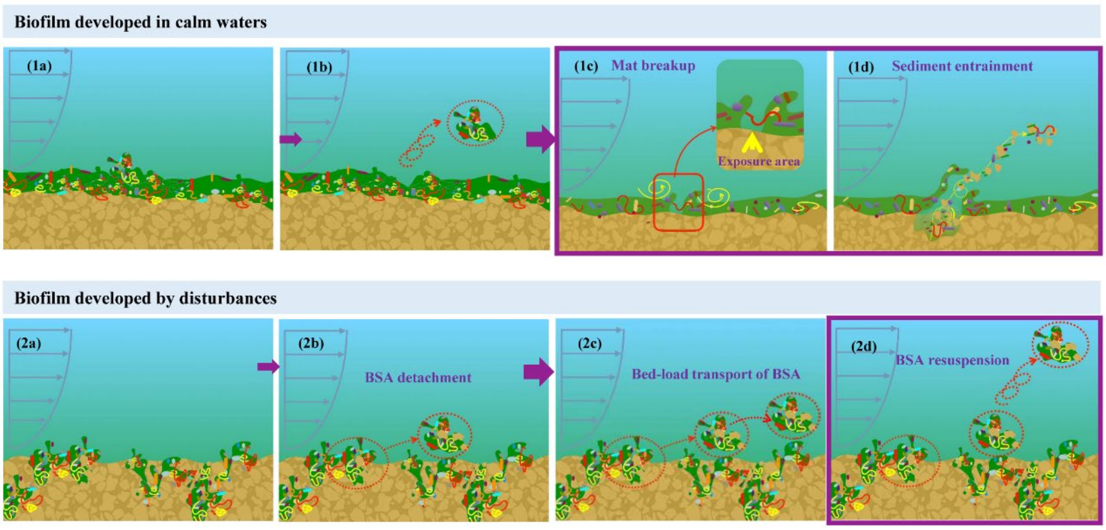

Figure 3. Schematic illustrations of the entrainment processes of biofilm mediated sediments developed in calm waters (1a-d) and under disturbance (2a-d). In calm waters, mat matrices of biofilm armour the underlying sediments (1a). Sediment resuspension follows surface organic-rich matter removal at a relatively moderate flow intensity, where the integrity of mat is not destroyed (1b), and the subsequent break-up of local mat (1c) and mass entrainment of underlying sediments (1d). The latter two processes occurred almost simultaneously and are included in one purple box. In disturbed environments, no mat matrices of biofilms were established, and discrete BSAs form fluffy appearance of sediment-water interfaces (2a). Sediment

entrainment follows BSA detachment at a relatively moderate flow intensity (2b), bed-load transport of the detached BSA (2c) and BSA suspension (2d).

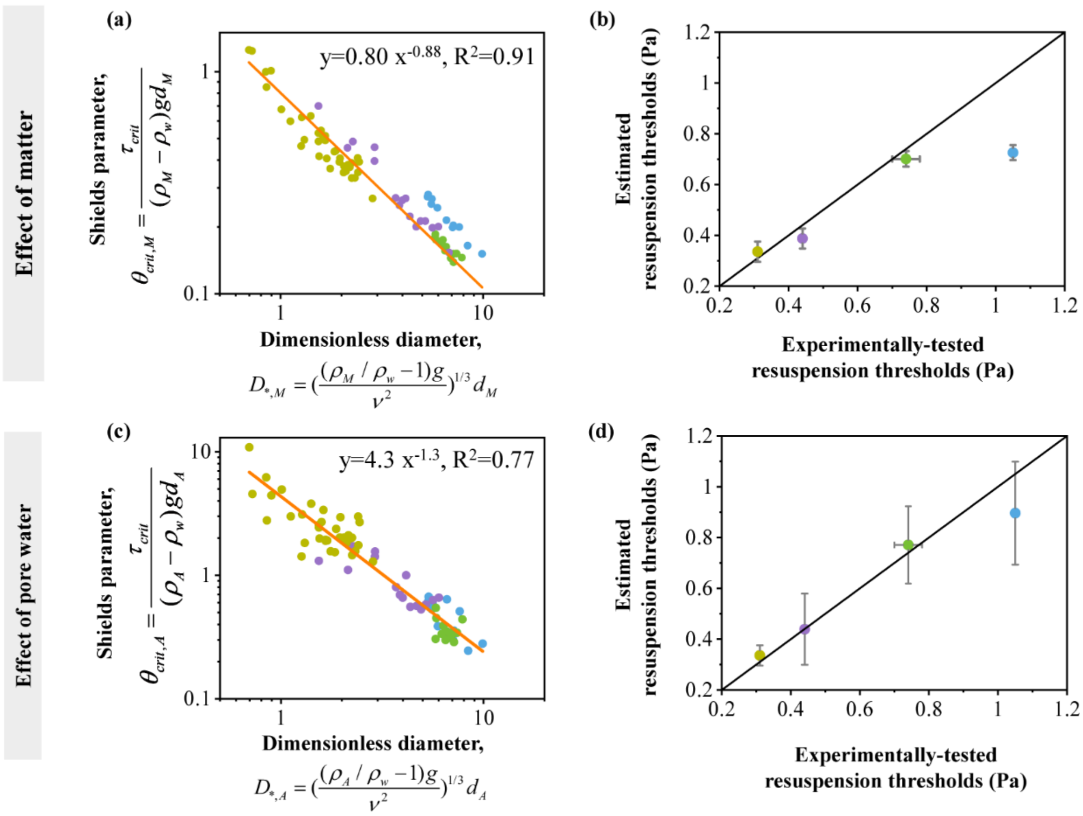

Figure 4. Plots of critical Shields parameter, against matter dimensionless diameter, to determine the effects of organic and inorganic particles on the resuspension of biofilm mediated sediments (a). The estimated resuspension threshold using the power law relationship presented in (a) are plotted against experimentally-tested resuspension thresholds for both the laboratory-created and field-collected, disturbed BSAs in (b). Plots of Shields parameter for aggregates against aggregate dimensionless diameter determine the effects of pore water (c). The estimated resuspension threshold using the power law relationship presented in (c) are plotted against the experimentally-tested thresholds in (d). All the BSAs established under disturbed conditions, including clay, fluff, silty and sandy field BSAs, are represented

as yellow, green, purple and blue dots, respectively. Results are represented as mean ± SD.

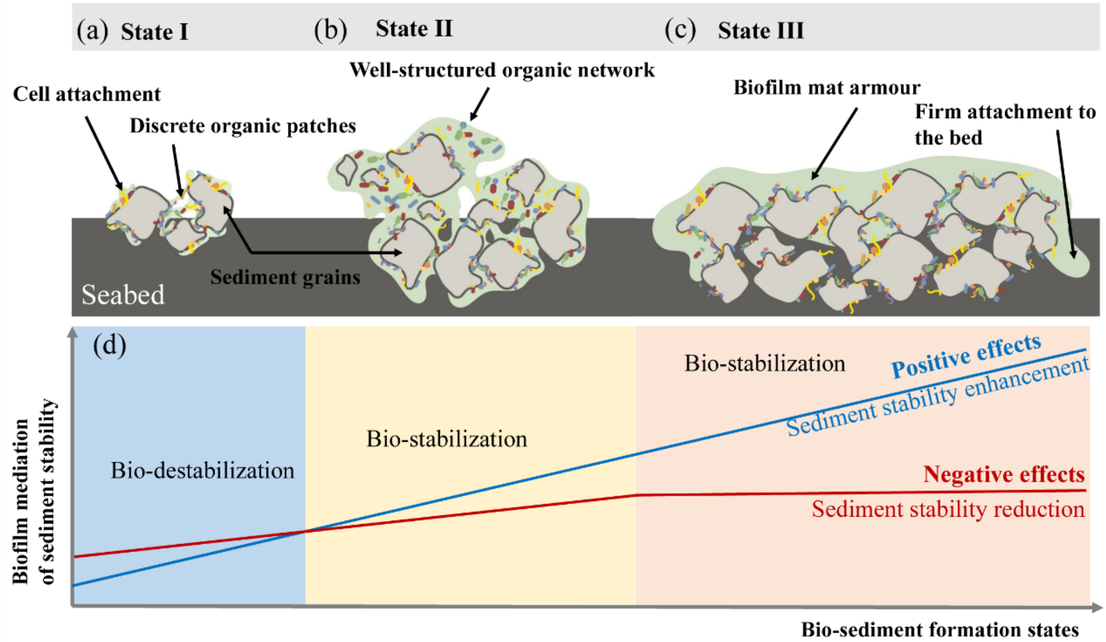

Figure 5. A conceptual framework that characterizes three states of bio-sediment formation. Distinct microstructures establish at each state (a-c). The biofilm growth and bio-sediment formation have two opposing effects on sediment stability and the net effects that determine bio-stabilization and destabilization vary at each state (d).